Fiber-Coupled Cavity-QED Source of Identical Single Photons

H. Snijders, J. A. Frey, J. Norman, V. P. Post, A. C. Gossard, J. E. Bowers, M. P. van Exter, W. Löffler, and D. Bouwmeester

Phys. Rev. Applied **9**, 031002 — Published 28 March 2018

DOI: 10.1103/PhysRevApplied.9.031002

A fiber coupled cavity QED source of identical single photons

H. Snijders,[1] J. A. Frey,[2] J. Norman,[3] V. P. Post,[1] A. C. Gossard,[3] J. E. Bowers,[3] M. P. van Exter,[1] W. Löffler,[1,*] and D. Bouwmeester[1,2]

[1] *Huygens-Kamerlingh Onnes Laboratory, Leiden University, P.O. Box 9504, 2300 RA Leiden, The Netherlands*

[2] *Department of Physics, University of California, Santa Barbara, California 93106, USA*

[3] *Department of Electrical & Computer Engineering, University of California, Santa Barbara, California 93106, USA*

We present a fully fiber coupled source of high-fidelity single photons. This is achieved by embedding an InGaAs semiconductor quantum dot in an optical Fabry-Perot micro cavity with robust design and rigidly attached single mode fibers which enables through-fiber cross polarized resonant laser excitation and photon extraction. Even without spectral filtering, we observe that the incident coherent light pulses are transformed into a stream of single photons with high purity (97%) and indistinguishability (90%), which is measured at an in-fiber brightness of 5% with an excellent cavity mode to fiber coupling efficiency of 85%. Our results pave the way for fully fiber integrated photonic quantum networks, further, our method is equally applicable for fiber coupled solid-state cavity-QED based photonic quantum gates.

Every isolated two-level quantum system such as an atom, ion, color center or quantum dot, can in principle be turned in a bright single photon source [1, 2]. Ideally, such a source produces a stream of single photons, never more or less than one photon per time bin, and all having the same Fourier limited spectrum and timing. Such a source would be essential for exploration of numerous quantum technologies such as optical quantum computing [3–6] and simulation [7]. Further, the reduced fluctuations of such single-photon light would enable exciting opportunities everywhere where noise is a limiting factor, in fields from metrology to microscopy.

However, only very recently, high-fidelity single photon sources have been demonstrated [8–13] that simultaneously fulfill the key requirements: near-unity single-photon purity and indistinguishability of consecutively emitted photons, and a high brightness. For a single photon source, high brightness and on-demand availability is crucial for efficient implementation of quantum photonic protocols. Additionally, to exploit the power of quantum interference, consecutively produced photons need to be indistinguishable, meaning that their wave functions must overlap well. Until recently, heralded spontaneous parametric down conversion sources [14] were the state of the art for single photon sources (SPS) [15], with which most quantum communication and optical quantum computing protocols have been demonstrated [16]. The main problem of these sources is that the Poissonian statistics of the generated twin photons will always result in a trade-off between single-photon purity (the absence of N>1 photon number states) and brightness (the probability to obtain a photon per time slot).

One way to deterministically produce single photons is to use trapped atoms [17], where single photon rates up to around 100 kHz have been obtained recently [18]. In order to enable integration and increasing the photon rate, solid-state systems have been investigated, in particular promising are semiconductor quantum dots (QDs) [1, 19, 20]. QDs have nanosecond-lifetime transitions that enable GHz rate production of single photons as required for numerous quantum technologies. Compared to other solid state emitters such as NV centers, nanowire QDs, excitons in carbon nanotubes or two-dimensional materials [21, 22], self-assembled QDs in cavities can show almost perfect purity and indistinguishability [9]. A challenging task is to couple the quantum emitter to propagating optical modes with near-unity efficiency. This can be achieved by placing them in optical micro cavities, which additionally increases the emission rate by cavity-QED Purcell enhancement, such as micropillar cavities [1, 23], photonic crystal cavities [24], or ring resonators [25].

For the next major step in implementing quantum dot single photon sources in complex photonic quantum networks, coupling to a single mode optical fiber is essential. Several challenges are connected to this: cryogenic compatibility [26], resonant optical pumping, high coupling efficiency and robust and stable polarization control. Only recently, a first study on a nonresonantly pumped multi mode fiber coupled device appeared [27]. Another approach is to employ fiber-tip micro cavities but the photon collection efficiency is limited to about 10% to date [28, 29].

Here, we show a prototype of a fully fiber coupled solid-state resonantly pumped and transmission-based source of identical photons. Our fiber coupled single photon device is sketched in Fig. 1: The device consists of a layer of self-assembled InAs/GaAs QDs embedded in a micropillar Fabry–Perot cavity (maximum Purcell factor $F_p = 11.2$) grown by molecular beam epitaxy [30]. The QD layer is embedded in a P–I–N junction, separated by a 27 nm thick tunnel barrier from the electron reser-

* loeffler@physics.leidenuniv.nl

voir to enable tuning of the QD resonance frequency by the quantum-confined Stark effect. Since we do not use air-guided micropillars but an oxide aperture for 3D confinement [31, 32], the device is very robust and the optical or quantum dot properties do not degrade by attachment of the fibers. It also allows for precise alignment of the fibers, and therefore the use of single-mode fibers. This is essential not only for integration in larger quantum networks, but also to enable high-fidelity polarization control as we show here.

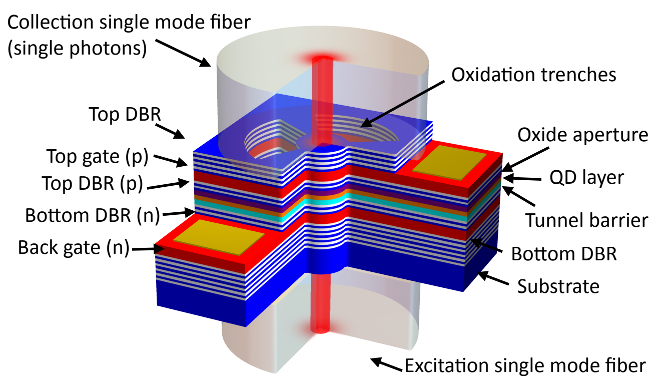

Figure 1. Sketch of the micro-cavity quantum dot device with attached fibers from bottom (excitation fiber) and top (single photon collection fiber). The trenches are used for wet-chemical oxidation of a sacrificial AlAs layer to form an intra-cavity lens or aperture that leads to transverse confinement of the optical cavity mode.

Single-mode fibers are attached to the front and back of the sample using a UV-curable Norland optical adhesive 81. The collection fiber is aligned to the cavity mode by making use of an inverted microscope. The sample is imaged by sending through the fiber light from a Superlum 471-HP2 superluminescent diode with a broad (900-980 nm) spectrum. The micropillar trenches are observed with a CCD camera allowing for coarse alignment of the fiber to the center of the micropillar. Fine alignment is done by bringing the fiber closer to the sample and detecting the resonantly transmitted light with a 1 m grating spectrometer. The optimal position is found by maximizing the fundamental mode of the cavity and reducing the transmission of the higher order modes. After UV curing the optical adhesive at the fiber tip, the fiber is attached to the copper mount with Stycast for stability. The excitation fiber is aligned by sending broadband light through the cavity via the now-attached collection fiber, and by maximizing the signal (see Supplemental Material [33] Section 1).

The cavity mode of our device has at the front surface a waist of $\omega_{front} = 2.14 \pm 0.08\,\mu\text{m}$ and at the back a waist of $\omega_{back} = 28.48 \pm 1.02\,\mu\text{m}$ at around 955 nm [31]. The increased waist at the back of the sample is due to the $650\,\mu\text{m}$ thick GaAs wafer. The fibers (Thorlabs 780HP) have a core radius of $2.2\,\mu\text{m}$ and 0.13 NA, which results in a mode waist of $\omega_{fiber} = 2.95 \pm 0.25\,\mu\text{m}$. Neglecting the phase and only taking into account the mode waist of the fiber, we have at the front side of the cavity a coupling efficiency of [34]

$$\eta = \left(\frac{2\omega_{fiber}\,\omega_{front}}{\omega_{fiber}^2 + \omega_{front}^2}\right)^2 \exp\left(-\frac{2u^2}{\omega_{fiber}^2 + \omega_{front}^2}\right).$$

Here, u is the transverse misalignment. Setting $u = 0$ we obtain an optimal efficiency of $\eta_{front} = 90\% \pm 7.6\%$. Experimentally, we obtain for our device a coupling efficiency that is very close to this value ($85 \pm 11\%$, see Supplemental Material [33] Section 7), confirming the high performance of the fiber attachment method. The fiber at the back of the sample has a reduced incoupling efficiency of 0.6% due to the thick GaAs substrate. For operation of our single photon source this reduced coupling efficiency is irrelevant because we excite the system from the back where the coupling efficiency only affects the required excitation laser power.

Now, we discuss the optical properties of the device, in all experiments presented here we investigate resonance fluorescence at a temperature of 5 K. The fundamental cavity mode is split in two linearly polarized modes, the H and V mode, induced by a small ellipticity of the cavity cross-section and material birefringence. Similarly, the neutral exciton transition of the QD is split in two linearly polarized transitions by the fine structure exchange interaction. Fig. 2a shows a false color plot of the transmission as a function of the applied bias voltage and laser frequency. Using a free-space polarizer and a fiber polarization controller, the input polarization is set along the H cavity polarization axes. The transmitted light is sent to a single photon detector. The two fine structure split QD transitions are clearly visible as dips in the transmission spectrum that shift as a function of the applied electric field. A cross sectional plot of Fig. 2a (grey line) is shown in Fig. 2c (red line). The depth of the dips indicate that the “X” QD transition couples more efficiently to the H cavity mode than the “Y” QD transition. This is confirmed by comparison to a numerical model[35, 36] taking all relevant cavity-QED and polarization effects into account (Supplemental Material [33] Section 3). From this model we also determine the angle θ between the X QD axis and the H cavity mode axis to be $\theta = 17°$, and the polarization splitting of the fundamental cavity mode (18 GHz).

Fig. 2b and c (blue line) show single photons that are filtered from the transmitted light with a combination of a fiber polarization controller and a free-space optical polarizer set to extinguish the transmitted laser light (cross polarization). We excite the system along the H cavity mode polarization but detect only photons emitted from the V-polarized cavity mode. This is ideal for efficient collection of the single photons that are coherently scattered from the Y-transition of the QD, as is seen in Fig. 2b. This is a workable scheme because for excitation of the QD-cavity system, we can simply remedy the reduced

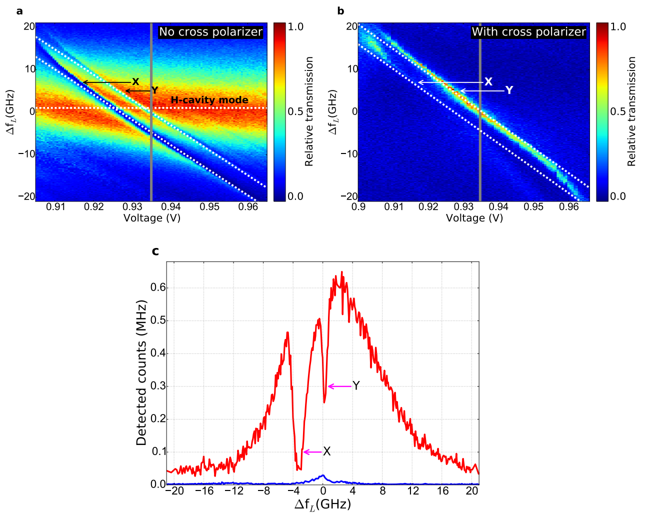

Figure 2. (a, b) False color plots of resonant transmission as a function of laser frequency and gate voltage. In (a), the incident laser light is polarized along the H cavity axis, and the transmitted light is detected without polarization selection. In (b), the remnant laser light is filtered out using a crossed polarizer oriented along the V-polarized cavity mode, to select the photons coherently scattered from the Y-transition of the QD. Panel (c) shows cross sectional plots (red line: without polarization selection, blue line: with crossed polarizer, scan time 1 s) at a gate voltage of 0.935 V, indicated by the grey line in (a) and (b). The X and Y QD transitions and the H-polarized cavity mode are labelled.

coupling of the Y QD transition to the H-polarized cavity mode by increasing the laser power, while the emitted single photons are efficiently collected by the V-polarized cavity mode. This also means that the Y QD transition is well suited to be used as a single photon source if it is resonantly excited, and, since the X transition can be neglected due to sufficient QD fine structure splitting, it resembles a nearly perfect two-level system.

We now investigate the dependency between maximum single photon rate and single photon purity that is achievable with the present device. For this, we first perform continuous-wave resonant spectroscopy experiments with a single frequency diode laser. We measure the second order correlation $g^2(\Delta\tau = 0)$ and the flux of emitted photons as a function of the incident laser power (Fig. 3a & b). In the correlation measurements, we observe a lower limit of $g^2(0) \approx 0.3$, which is due to limited timing accuracy due to detector jitter; this is confirmed by comparing to reference measurements using short laser pulses (see Supplemental Material [33] Section 4). Further, we observe an increase in $g^2(0)$ with increasing laser power. Two-photon emission from a single quantum system should in principle be absent if it is excited with laser pulses much shorter than its lifetime. We suspect imperfect laser extinction, which should also be visible in the detected photon count rate, shown in Fig. 3b: instead of a simple saturation behav-

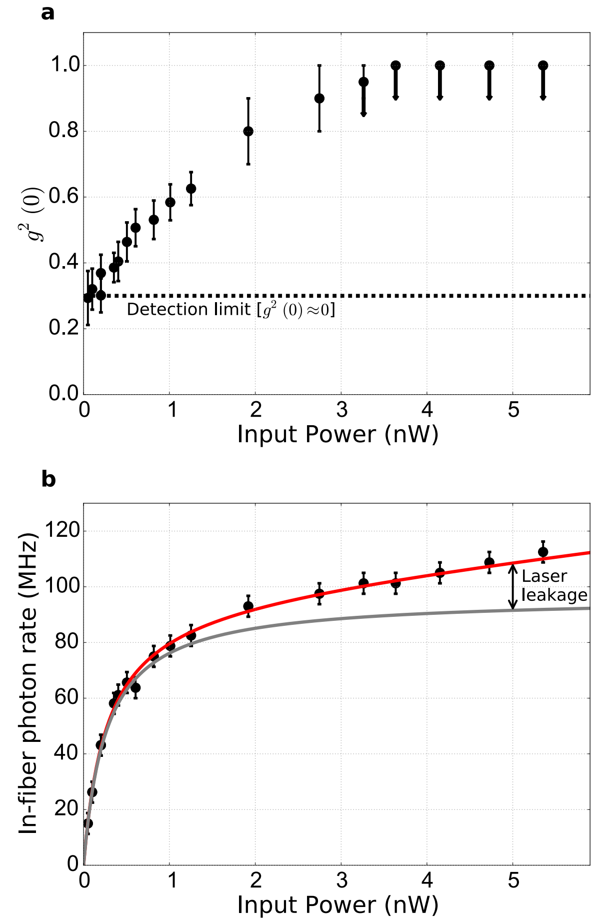

Figure 3. Measurement of the second order correlation function $g^2(0)$ versus the incident laser power under continuous-wave excitation (a). The dashed line indicates the approximate limit on g^2 set by the detector jitter (two-detector instrument response function full width ≈ 532 ps, see Supplemental Material [33] Section 4 for details). (b) Simultaneously measured single photon rate (corrected for detection efficiency). The fit (red line) takes into account the saturation of the QD transition (grey line), as well as residual laser light due to non-perfect polarization extinction.

ior of the count rate as a function of input laser power P, we observe an additional linear background. We find that the photon rate can very well be fitted (red line) by $96.0\,\text{MHz}/(1+0.26\,\text{nW}/P)+3.39\,\text{MHz}\cdot\text{nW}^{-1}\times P$, where the first part describes standard two-level system saturation [37] and is plotted separately with the grey line in Fig. 3b, and the saturation power agrees well to previous results on similar devices [38]. The power-linear term is most likely due to imperfect polarization extinction of the exciting laser light. These measurements show that good single-photon performance is expected for an input power well below a nW.

For quantum photonic applications, single photons are required on-demand with precise timing. We realize this using a resonant (around 932.58 nm) pulsed laser with

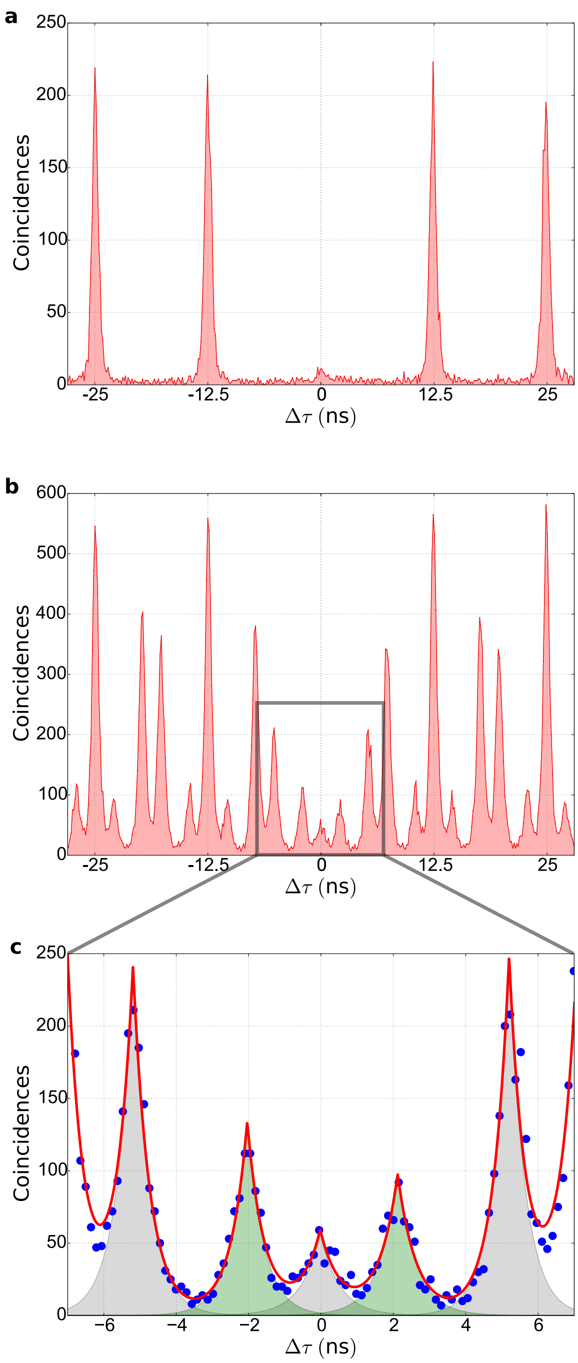

Figure 4. Photon correlations of the QD transition under pulsed excitation. (a): second-order correlation measurement, where $g^2(0) = 0.037$ is obtained from the integrated photon counts in the zero time delay peak divided by the average of the adjacent four peaks. (b): Photon indistinguishability measurement for consecutive photons 5.2 apart. A magnified view around $\Delta\tau = 0$ and a double exponential fit of this data is shown in (c). Taking into account $g^2(0) = 0.037$ we obtain a measured indistinguishability of $M = 0.90$. Measurement time: 600 s (a), 1200 s (b, c).

20 ps pulse length and 12.5 ns period. These values are well-matched to the quantum dot transition in the cavity as shown in Fig. 2c. Using a pulsed laser, we are no longer limited by the jitter of the single photon detectors and can obtain a more accurate value for $g^2(0)$. At a sufficient low power of 100 pW, we measure a second order correlation of $g^2(0) = 0.037 \pm 0.012$ as shown in Fig. 4a. Note that we did not use spectral filtering of the cavity emitted light, in contrast to previous investigations [9]. As we have investigated above, $g^2(0)$ is in our case most likely limited by imperfect extinction of the excitation laser light.

Next we determine the indistinguishability of two successively produced single photons. For this, we send the emitted (single) photons into a fiber-based Mach-Zehnder interferometer where one arm introduces a delay of 5.2 ns. In order to create two excitation-laser pulses with exactly the same delay of 5.2 ns, we use a non-interferometric Michelson-type setup with adjustable delay. As a result, consecutively emitted photons arrive simultaneously at the final fiber splitter. We again measure photon correlations between both output ports (Supplemental Material [33] Section 2). If two consecutively produced single photons are indistinguishable, they will undergo quantum interference and "bunch", i.e. two-photon coincidences at $\tau = 0$ are expected to be absent in the ideal case. This can be seen in Fig. 4b, in particular if compared to the case where the photons are made distinguishable artificially (Supplemental Material [33] Section 5). By fitting the data with double exponential functions and taking into account a finite value of $g^2(0) = 0.037 \pm 0.012$ as well as imperfect fiber splitting ratios, we obtain an indistinguishability of $M = 0.90 \pm 0.05$ (Fig. 4c). The deviation from $M = 1$ might be due to residual spectral diffusion or nuclear-spin induced dephasing mechanisms. Finally, to determine the brightness of the device, i.e. the fraction that each laser pulse produces a single photon in the detection fiber, we carefully characterize our setup including optical loss and detector efficiencies, see Supplemental Material [33] Section 6, and we obtain an in-fiber brightness of 0.05 ± 0.01 photons per laser pulse. The reduced value is due to an imperfect spectral alignment of the QD and cavity mode, while the fiber coupling efficiency is excellent at 85%, or 94% of its optimum.

In conclusion, we have shown a prototype of a fully fiber coupled solid-state single photon source that produces on-demand single photons with a purity of 0.96 ± 0.01, indistinguishability of 0.90 ± 0.05 and a brightness of 0.05 ± 0.01, with fiber coupling efficiency of 0.85 ± 0.11. These figures are already promising for exploring small optical fiber based quantum networks such as for boson sampling. From another point of view, we have demonstrated a first all-fiber integrated cavity-QED based photonic quantum gate that filters out single photons from pulses of coherent laser light. A next step is charging of the QD with a single electron or hole spin to create a quantum memory [39] which makes the device usable as a quantum node for remote entanglement generation, quantum key distribution, and distributed quantum computation.

ACKNOWLEDGMENTS

We thank D. Kok and M.F. Stolpe for fruitful discussions. We acknowledge funding from FOM-NWO (08QIP6-2), from NWO/OCW as part of the Frontiers of Nanoscience program, and from the National Science Foundation (NSF) (0901886, 0960331).

[1] Santori, C., Fattal, D., Vučković, J., Solomon, G. S. & Yamamoto, Y. Indistinguishable photons from a single-photon device. *Nature* **419**, 594 (2002).

[2] Yamamoto, Y., Kim, J., Benson, O. & Kan, H. A single-photon turnstile device. *Nature* **397**, 500 (1999).

[3] Knill, E., Laflamme, R. & Milburn, G. J. A scheme for efficient quantum computation with linear optics. *Nature* **409**, 46 (2001).

[4] Kok, P., Munro, W. J., Nemoto, K., Ralph, T. C., Dowling, J. P. & Milburn, G. J. Linear optical quantum computing with photonic qubits. *Reviews of Modern Physics* **79**, 135 (2007).

[5] Varnava, M., Browne, D. E. & Rudolph, T. How Good Must Single Photon Sources and Detectors Be for Efficient Linear Optical Quantum Computation? *Phys. Rev. Lett.* **100**, 060502 (2008).

[6] O'Brien, J. L., Furusawa, A. & Vučković, J. Photonic quantum technologies. *Nat. Photonics* **3**, 687 (2009).

[7] Aspuru-Guzik, A. & Walther, P. Photonic quantum simulators. *Nat. Phys.* **8**, 285 (2012).

[8] Gazzano, O., Michaelis de Vasconcellos, S., Arnold, C., Nowak, A., Galopin, E., Sagnes, I., Lanco, L., Lemaître, A. & Senellart, P. Bright solid-state sources of indistinguishable single photons. *Nat. Commun.* **4**, 1425 (2013).

[9] Somaschi, N., Giesz, V., De Santis, L., Loredo, J. C., Almeida, M. P., Hornecker, G., Portalupi, S. L., Grange, T., Antón, C., Demory, J., Gómez, C., Sagnes, I., Lanzillotti-Kimura, N. D., Lemaítre, A., Auffeves, A., White, A. G., Lanco, L. & Senellart, P. Near-optimal single-photon sources in the solid state. *Nat. Photonics* **10**, 340 (2016).

[10] Ding, X., He, Y., Duan, Z.-C., Gregersen, N., Chen, M.-C., Unsleber, S., Maier, S., Schneider, C., Kamp, M., Höfling, S., Lu, C.-Y. & Pan, J.-W. On-Demand Single Photons with High Extraction Efficiency and Near-Unity Indistinguishability from a Resonantly Driven Quantum Dot in a Micropillar. *Phys. Rev. Lett.* **116**, 020401 (2016).

[11] Aharonovich, I., Englund, D. & Toth, M. Solid-state single-photon emitters. *Nat. Photonics* **10**, 631 (2016).

[12] He, Y.-M., Liu, J., Maier, S., Emmerling, M., Gerhardt, S., Davanço, M., Srinivasan, K., Schneider, C. & Höfling, S. Deterministic implementation of a bright, on-demand single-photon source with near-unity indistinguishability via quantum dot imaging. *Optica* **4**, 802 (2017).

[13] Burek, M. J., Meuwly, C., Evans, R. E., Bhaskar, M. K., Sipahigil, A., Meesala, S., Machielse, B., Sukachev, D. D., Nguyen, C. T., Pacheco, J. L., Bielejec, E., Lukin, M. D. & Lončar, M. Fiber-Coupled Diamond Quantum Nanophotonic Interface. *Physical Review Applied* **8**, 024026 (2017).

[14] Barz, S., Cronenberg, G., Zeilinger, A. & Walther, P. Heralded generation of entangled photon pairs. *Nat. Photonics* **4**, 553 (2010).

[15] Eisaman, M. D., Fan, J., Migdall, A., Polyakov, S. V. & Fan, J. Invited Review Article: Single-photon sources and detectors. *Rev. Sci. INSTRUMENTS* **82**, 071101 (2011).

[16] Takemoto, K., Nambu, Y., Miyazawa, T., Sakuma, Y., Yamamoto, T., Yorozu, S. & Arakawa, Y. Quantum key distribution over 120 km using ultrahigh purity single-photon source and superconducting single-photon detectors. *Sci. Rep.* **5**, 14383 (2015).

[17] Kuhn, A., Hennrich, M. & Rempe, G. Deterministic Single-Photon Source for Distributed Quantum Networking. *Phys. Rev. Lett.* **89**, 067901 (2002).

[18] Higginbottom, D. B., Slodička, L., Araneda, G., Lachman, L., Filip, R., Hennrich, M. & Blatt, R. Pure single photons from a trapped atom source. *New J. Phys.* **18**, 093038 (2016).

[19] Bennett, A. J., Lee, J. P., Ellis, D. J. P., Farrer, I., Ritchie, D. A. & Shields, A. J. A semiconductor photon-sorter. *Nat. Nanotechnol.* **11**, 857 (2016).

[20] Hennessy, K., Badolato, A., Winger, M., Gerace, D., Atatüre, M., Gulde, S., Fält, S., Hu, E. L. & Imamoğlu, A. Quantum nature of a strongly coupled single quantum dot–cavity system. *Nature* **445**, 896 (2007).

[21] Rogers, L. J., Jahnke, K. D., Teraji, T., Marseglia, L., Müller, C., Naydenov, B., Schauffert, H., Kranz, C., Isoya, J., McGuinness, L. P. & Jelezko, F. Multiple intrinsically identical single-photon emitters in the solid state. *Nat. Commun.* **5**, 4739 (2014).

[22] Sipahigil, A., Jahnke, K., Rogers, L., Teraji, T., Isoya, J., Zibrov, A., Jelezko, F. & Lukin, M. Indistinguishable Photons from Separated Silicon-Vacancy Centers in Diamond. *Phys. Rev. Lett.* **113**, 113602 (2014).

[23] Snijders, H., Frey, J. A., Norman, J., Bakker, M. P., Langman, E. C., Gossard, A., Bowers, J. E., van Exter, M. P., Bouwmeester, D. & Löffler, W. Purification of a single-photon nonlinearity. *Nat. Commun.* **7**, 12578 (2016).

[24] Müller, K., Rundquist, A., Fischer, K. A., Sarmiento, T., Lagoudakis, K. G., Kelaita, Y. A., Sánchez Muñoz, C., Del Valle, E., Laussy, F. P. & Vučković, J. Coherent generation of nonclassical light on chip via detuned photon blockade. *Phys. Rev. Lett.* **114**, 1 (2014).

[25] Davanco, M., Liu, J., Sapienza, L., Zhang, C. Z., De Miranda Cardoso, J. V., Verma, V., Mirin, R., Nam, S. W., Liu, L. & Srinivasan, K. Heterogeneous integration for on-chip quantum photonic circuits with single quantum dot devices. *Nat. Commun.* **8**, 1 (2017).

[26] Haupt, F., Oemrawsingh, S. S. R., Thon, S. M., Kim, H., Kleckner, D., Ding, D., Suntrup III, D. J., Petroff, P. M. & Bouwmeester, D. Fiber-connectorized micropillar cavities. *Appl. Phys. Lett* **97**, 131113 (2010).

[27] Schlehahn, A., Fischbach, S., Schmidt, R., Kaganskiy, A., Strittmatter, A., Rodt, S., Heindel, T. & Reitzenstein, S. A stand-alone fiber-coupled single-photon source (2017). arXiv: 1703.10536.

[28] Muller, A., Flagg, E. B., Metcalfe, M., Lawall, J. & Solomon, G. S. Coupling an epitaxial quantum dot to

a fiber-based external-mirror microcavity. *Appl. Phys. Lett.* **95**, 173101 (2009).

[29] Greuter, L., Starosielec, S., Kuhlmann, A. V. & Warburton, R. J. Towards high-cooperativity strong coupling of a quantum dot in a tunable microcavity. *Phys. Rev. B* **92**, 045302 (2015).

[30] Strauf, S., Stoltz, N. G., Rakher, M. T., Coldren, L. A., Petroff, P. M. & Bouwmeester, D. High-frequency single-photon source with polarization control. *Nat. Photonics* **1**, 704 (2007).

[31] Bonato, C., Gudat, J., de Vries, K., Thon, S. M., Kim, H., Petroff, P. M., van Exter, M. P. & Bouwmeester, D. Optical modes in oxide-apertured micropillar cavities. *Opt. Lett.* **37**, 4678 (2012).

[32] Bakker, M. P., Barve, A. V., Zhan, A., Coldren, L. A., van Exter, M. P. & Bouwmeester, D. Polarization degenerate micropillars fabricated by designing elliptical oxide apertures. *Appl. Phys. Lett.* **104**, 151109 (2014).

[33] See Supplemental Material at [URL will be inserted by publisher] for extended analysis.

[34] Ghatak, K. & Thyagarajan, A. *An introduction to fiber optics* (Cambridge University Press, 1998).

[35] Johansson, J., Nation, P. & Nori, F. QuTiP: An open-source Python framework for the dynamics of open quantum systems. *Comput. Phys. Commun.* **183**, 1760 (2012).

[36] Johansson, J. R., Nation, P. D. & Nori, F. QuTiP 2: A Python framework for the dynamics of open quantum systems. *Comput. Phys. Commun.* **184**, 1234 (2013).

[37] Loudon, R. *The Quantum Theory of Light (Oxford Science publications)* (Oxford University Press, USA, 1973), 3rd ed edn.

[38] Bakker, M. P., Snijders, H., Löffler, W., Barve, A. V., Coldren, L. A., Bouwmeester, D. & van Exter, M. P. Homodyne detection of coherence and phase shift of a quantum dot in a cavity. *Opt. Lett.* **40**, 3173 (2015).

[39] Kroutvar, M., Ducommun, Y., Heiss, D., Bichler, M., Schuh, D., Abstreiter, G. & Finley, J. J. Optically programmable electron spin memory using semiconductor quantum dots. *Nature* **432**, 81 (2004).